ORIGINAL ARTICLE

lajss.org© Latin American Journal of Solids and Structures

www.lajss.org

Scaling of An Impacted Reticulated Dome Using Partial Similitude Method

Demin Wei[a]

Chenxi Hu[a]*

[a] School of Civil Engineering and Transportation, South China University of Technology, China. Email: dmwei@scut.edu.cn, maradonan2@sina.com

*Corresponding author

http://dx.doi.org/10.1590/1679-78255342

Abstract

Strain-rate effects can distort model testing with geometrically-similar models. In impact modelling this problem is usually addressed by revising the impact conditions, but such kind of method is inadequate for modelling impact on a reticulated dome. A new technique was proposed and tested. Apart from adjusting the impact conditions, the technique adds additional mass to components of the model to balance the strain-rate effects. That allows studying in model scale more complex structures in which the strain rate varies over the structure's components. Model scale tests of impact on a reticulated dome showed good agreement with full scale in terms of displacements and axial forces on the structure's rods. Those results verify the effectiveness of the new technique.

Keywords:

Reticulated Domes; Scaling Laws; Strain-rate Effects; Impact; Model Testing.

1 INTRODUCTION

Accidents and explosions causing damage are a matter of growing concern in civil engineering after the 9/11 terrorist attacks. The dynamic response of reticulated domes subjected to impact loading has been investigated theoretically and experimentally in recent years (Wang X. et al, 2016; Lin L. et al, 2015; Wei D. and Hu C., 2015; Wu C. et al, 2014; Wang X. and Lei J., 2012; Zheng L., 2012; Zheng L. and Chen Z., 2011; Fan F. et al, 2010). In order to validate either theoretical or numerical results, experiments are indispensable. They are, however, always carried out on scaled-down models so as to be efficient and cost-effective. Indeed, for large-span structures such as the reticulated dome to be discussed here, a full-size model test would be impossibly large. Generally the dynamic response of prototypes can be predicted adequately by scaled-down model tests and through applying scaling laws (Ding B. et al, 2015; Wang D. et al, 2011; Li H. et al, 2006).

Scaling laws for impacted structures have been investigated continuously. Johnson (1972) has used a dimensionless damage number D_n to identify various impact regions in metals. Zhao (1998) improved this number by taking into account the geometrical effects and applied it to the dynamic response of simple impacted structures. The derivation of these numbers are based on a set of governing equations. However, it is always difficult to deduce the dimensionless numbers through theoretical equations. A more general method for the scaling of impacted structure is dimensional analysis (Buckingham E., 1914; Westine P. S. et al, 1973), by which Nevill (1963) and Duffey (1970) achieved scaling laws for structures subjected to explosion, impact and thermal loading.

Suppose that the small-scale model and the full-scale prototype are made of the same material and that the scaling factor of the model is γ_l. Simple dimensional analysis shows that the ratio of model strain to prototype strain γ_ε is one to one, which leads to a unit ratio of the stress γ_σ. Jones (2011) has detailed the analysis procedure and he

Received October 25, 2018. In revised form November 23, 2018. Accepted December 08, 2018. Available online December 10, 2018.
http://dx.doi.org/10.1590/1679-78255342

explains that these ratios constitute the geometrically similar scaling law. It is widely used in static and dynamic experiments. That classic law can, however, be distorted due to gravity, material strain-rate sensitivity and fracture (Xu Z. et al, 2016; Yang F. J. et al, 2013; Jackson K. E., 1994). Complete and perfect solutions for those kind of distortions are always impossible so that researchers resort to partial similar method or sequential method such as in references (Soedel W., 1971; Shokrieh M. M. and Askari A., 2013).

This study aimed at correcting the scaling laws to account for strain-rate effects. At the outset, express the dynamic stress σ_d on the prototype in the generic form of a material constitutive law as

$$\sigma_d = \sigma_s g(\dot{\varepsilon}) \tag{1}$$

where σ_s and $\dot{\varepsilon}$ denote the static stress and the stain rate. $g(\dot{\varepsilon})$ is a generic function of $\dot{\varepsilon}$ representing strain rate effects. If the prototype of the structure is geometrically scaled by γ_l, then its dynamic stress is written as

$$\sigma_d = \sigma_s g(\dot{\varepsilon}\gamma_l) \tag{2}$$

Apparently the dynamic stress ratio is not 1 contrary to the geometrically similar scaling law. In general, the model used to represent the prototype is smaller in the size for structural engineering experiments. However, the equations and method in this paper can also be applied to models larger than the prototype since γ_l can either be smaller or larger than 1, but the smaller case is considered in the paper. Non-scaling phenomena become even more obvious as the model's scale gets smaller or larger. This will result in underestimates or overestimates about the behaviour of the prototype, as can be seen in Norman Jones' (1987) experiments and Booth's et al. (1983) tests. Size effect in composite material behaviour for inelastic analysis are also highlighted in the works of Viot et al. (2008) and Wisnom (1999).

Drazetic et al. (1994) provided an inspiring way of dimensional analysis to correct non-scaling phenomenons. Alves & Oshiro (2006) further exploited this idea, and properly scaled strain rate sensitive models by correcting either initial speed or the mass of the impactor. Based on the idea of changing the impact velocity, Oshiro & Alves (2009) dealt with the scaling of structures subjected to impact loads when using a power law constitutive equation. Mazzariol & Alves (2014) developed a method to represent impacted structures using scaled models made of different materials with a combination of modifying velocity and mass of the impactor. However, as found in the research of our concerns, None of these methods are precise enough to describe complex structures, particularly for the reticulated shell concerned in this paper. Therefore, a new technique based on partial similarity and dimensional analysis is proposed here. The core manipulation of the technique is adding additional mass to components of the dome according to the developed scaling law to balance the strain-rate induced size effects. The amount of mass must be scaled such that the dimensionless number describing the dome's dynamic response is unchanged. At last, the technique is demonstrated by numerical analysis of the prototype and the models of an impacted reticulated dome.

2 SCALING METHOD

Since geometrically similar scaling (a law denoted as MI) is not suitable for strain rate-sensitive structures, dimensional analysis is needed to find a new dimensionless number on which to base the scaling law. Buckingham's (1914) π theorem is a useful dimensional analysis tool.

Seven variables must be considered to acquire the scaled input variables of the structure: the impacting mass M, the impact velocity V, a characteristic dimension of the structure *l*, material density *ρ*, response time t, dynamic stress σ_d and the strain ε. Input variables include the impact velocity, the mass of the impactor and the mass of components of the structure. [*l*], [σ_d] and [t] are a set of fundamental dimensions, hence the dimensionless π terms calculated through Buckingham π theorem are $\pi_1 = \mathrm{M}^{-1} l^3 \rho$, $\pi_2 = l^{-1}\mathrm{tV}$, $\pi_3 = \varepsilon$, $\pi_4 = \mathrm{M}^{-1} l \mathrm{t}^2 \sigma_d$

If the impact response of the model and the prototype are to be similar, their dimensionless numbers should be equal, specifically $\pi_{ip}=\pi_{im}$ (i=1,2,3,4) where ip and im denote the model and the prototype respectively. It can be deduced from $\pi_{2p}=\pi_{2m}$ and $\pi_{4p}=\pi_{4m}$ that

$$\gamma_M = \gamma_l^3 \gamma_V^{-2} \gamma_{\sigma_d}, \tag{3}$$

where γ is the scaling factor of the variable denoted by the subscript. For example, $\gamma_M=M_m/M_p$. It is reasonable to configure the material constitutive law in the general form of equation (1)

$$\sigma_d = \sigma_s g(\dot{\varepsilon}), \tag{1}$$

where $\dot{\varepsilon}$ is the strain rate. Scaling the variables of Equation (1) and substituting γ_{σ_d} into Equation (2) leads to

$$\gamma_M = \gamma_l^3 \gamma_V^{-2} \gamma_{\sigma_s} g(\dot{\varepsilon}_m) / g(\dot{\varepsilon}_p) \tag{4}$$

Strain rate for the prototype is related with that for the model according to the scaling of the model and the impact velocity as $\dot{\varepsilon}_p = \dot{\varepsilon}_m \gamma_l / \gamma_V$. Substituting this equation into Equation (4) results in

$$\gamma_M = \gamma_l^3 \gamma_V^{-2} \gamma_{\sigma_s} g(\dot{\varepsilon}_m) / g(\dot{\varepsilon}_m \gamma_l / \gamma_V) \tag{5}$$

from which it is easy to see the non-scaling of dynamic stress induced by strain rate effects. Practically, γ_l is chosen on purpose by researchers in the set of experiments. As a consequence, either the mass or the initial velocity of the impactor should be revised to balance Equation (5).

The general method of altering the impact conditions (denoted as MII) works well for scaling structures that deform with a constant strain rate. It is even applicable for situations in which the strain rate changes over the time provided that the average strain rate is properly selected. However, a more general situation is that the strain rate varies over different parts of an impacted structure at the same time, a situation impossible to deal with by only revising the impact conditions.

A solution for this involves taking a closer look at the equation $\pi_{1p}=\pi_{1m}$, which can be expressed as

$$\gamma_M = \gamma_l^3 \gamma_\rho = \gamma_l^3 \gamma_V^{-2} \gamma_{\sigma_s} g(\dot{\varepsilon}_m) / g(\dot{\varepsilon}_m \gamma_l / \gamma_V) \tag{6}$$

Reorganizing Equation (6) yields

$$\gamma_\rho = \gamma_V^{-2} \gamma_{\sigma_s} g(\dot{\varepsilon}_m) / g(\dot{\varepsilon}_m \gamma_l / \gamma_V) \tag{7}$$

which suggests that the density of the model's material should also be revised according to the strain rate.

From a structural mechanics point of view, the strain rate in Equation (5) is different from that in Equation (7). The scaling of the impactor's mass or its initial impact speed should be combined with an evaluation of the strain rate near the impact point. The material density of certain parts of the structure must be corrected based on the strain rate at that point. Equations (5) and (7) thus provide a more comprehensive understanding of the scale revision procedure. It will involve adjusting the impactor's mass or velocity to balance the strain rates in the impact region (whose displacements during structural responses are quite small thus can be neglected) and adjusting the material density of the model to balance the strain rates in the unimpacted region (whose displacements cannot be neglected). This new method is denoted as MIII. Apparently MII can be regarded as a reduced method of MIII.

Adjusting the impactor's mass is much more convenient than adjusting its impact velocity, since the latter needs iteration. As a result, mass adjustments were used in the following numerical analysis. In that case the scaling factor of impact velocity $\gamma_V=1$. In practice it is also difficult to alter the material's density while keeping other material properties unchanged. An alternative approach is to add additional mass to components of the model. For example, if components of the prototype are rod-shaped, then the scaling factor of components' mass per metre is $\gamma_m=\gamma_\rho\gamma_{Ap}$($A_p$ denotes section area of the rod). As a result, the added mass per metre Δm on rods of the model can be calculated as $\Delta m=\rho A_p(\gamma_\rho-1)$, which by Equation (7) lead to

$$\Delta m = \rho A_p \left[\gamma_v^{-2} \gamma_{\sigma_s} g(\dot{\varepsilon}_m) / g(\dot{\varepsilon}_m \gamma_l / \gamma_v) - 1\right] \tag{8}$$

where ρ specifically refers to the material density of components. It is important to note that the added mass should not provide any added strength to the model, so the material strength of any masses attached to the rods must be much lower than that of the model's material. This requirement ensures that the act of adding the mass is completely equivalent to altering the density of the material.

In summary, then, the complete scaling technique MIII for a structure subjected to impact is listed as follow:

I. Determine representative strain rate $\dot{\varepsilon}_m$ for different parts of the model.

II. Calculate the actual mass of the impactor in model scale according to Equation (6). Then calculate the mass that should be added to components according to Equation (8).

III. Estimate the dynamic response of the prototype according to the results with the model using revised scaling factors.

Step I is based on geometrically similar-model (MI) and $\dot{\varepsilon}_m$ is calculated as half of the maximum strain rate. This procedure was adopted according to Perrone and Bhadra (1979,1984).

Table 1: Scaling factors for MI, MII and MIII.

Scaling factor	MI	MII	MIII
γ_M	1	$\gamma_l^3\gamma_{\sigma_s} g(\dot{\varepsilon}_m)/g(\dot{\varepsilon}_m\gamma_l)$	$\gamma_l^3\gamma_{\sigma_s} g(\dot{\varepsilon}_m)/g(\dot{\varepsilon}_m\gamma_l)$
γ_V	1	1	1
γ_ρ	1	1	$\gamma_{\sigma_s} g(\dot{\varepsilon}_m)/g(\dot{\varepsilon}_m\gamma_l)$

The scaling factors are summarized in Table 1. It should be kept in mind that γ_ρ for MIII models is realized through adding additional mass in real tests, though with finite element modelling γ_ρ can be adjusted by simply revising the density of the material.

3 FINITE ELEMENT MODELLING

Consider the single-layer, reticulated dome shown in Figure 1 with a span L=40m and height H=8m. The dome's radius is R=29m. All 36 joints on the outer ring are hinged to the foundation. The dome is composed of hollow rods with a circular cross-section fabricated from Chinese steel Q235 (Ministry of Construction, 2014). The rods whose impact responses are to be discussed are labeled in Figure 1(c). They are rigidly connected by welded joints and can be divided into 3 categories depending on their direction. The outer radius of the radial rods is 73.0mm and their wall thickness is 4.5mm (Φ73.0×4.5). Using the same nomenclature the diagonal rods are Φ83.0×4.0 and the latitudinal rods are Φ63.5×5.5. The density of the steel is ρ=7850kg/m^3 and its elastic modulus E=206GPa. The Poisson's ratio μ=0.3. In simple tension, the yield limit σ_y and the ultimate strength σ_b of the material are 235MPa and 450MPa respectively. The mass impactor is assumed to strike the dome vertically at its apex with an impact speed V=30m/s. The impactor is a 370mm cube weighing M=400kg. The striking position and the striking direction is chosen to represent a typical condition of the impact. Such kind of impact is accepted as a benchmark of tests referring to (Wang X. et al, 2016; Lin L. et al, 2015; Wei D. and Hu C., 2015; Wu C. et al, 2014; Wang X. and Lei J., 2012; Zheng L., 2012; Zheng L. and Chen Z., 2011; Fan F. et al, 2010).

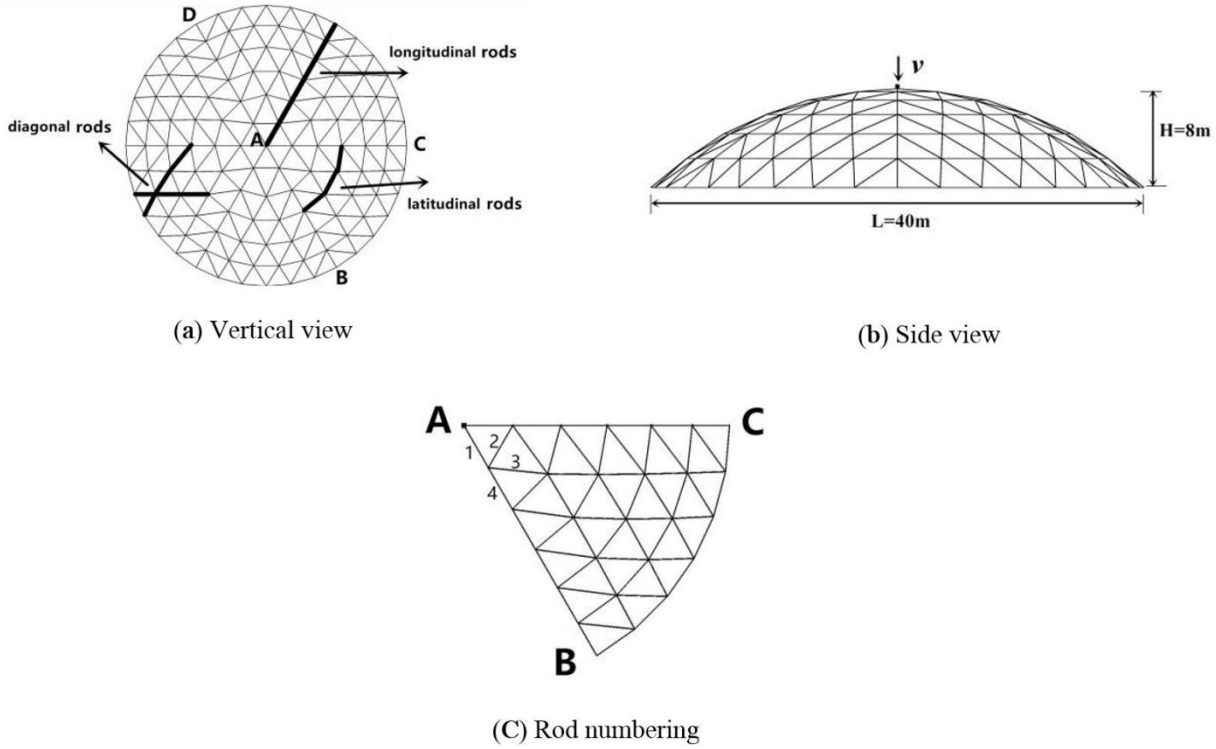

(a) Vertical view

(b) Side view

(C) Rod numbering

Figure 1: The single-layer lattice shell.

The dynamic response of the prototype and its scaled-down model are solved numerically using commercial FE package ANSYS/LS-DYNA. That allows easy comparison of geometrical scaling method (MI) with reduced scaling method (MII) and the proposed new method (MIII). The results with models designed according to these methods can be scaled up to predict the prototype's behaviour and the accuracy of their results can be compared. Models at 1/10, 1/20, 1/50 and 1/100 scale were prepared for this purpose, so the spans of the models were 4m, 2m, 0.8m and 0.4m respectively.

3.1 Material model

Piecewise linear plasticity model is chosen as the material constitutive law which is based on the well-known Cowper-Symonds constitutive equation (Cowper G. R. and Symonds P. S., 1957)

$$\sigma_d(\varepsilon,\dot{\varepsilon}) = \sigma_s(\varepsilon)\left[1+\left(\frac{\dot{\varepsilon}}{C}\right)^{\frac{1}{p}}\right] \tag{9}$$

where C and P are material constants. Typically C=40 and P=5 for the Q235 steel to be used in the prototype and the model. Strain rate here actually refers to plastic strain rate which causes the strain rate effects with the Cowper-Symonds constitutive law.

The adopted constitutive curve is presented in Figure 2. 7 interpolation points signaled in the figure are input into the programme: (0.000, 235), (0.003, 290), (0.007, 330), (0.018, 375), (0.040, 400), (0.100, 425), (0.200, 450).

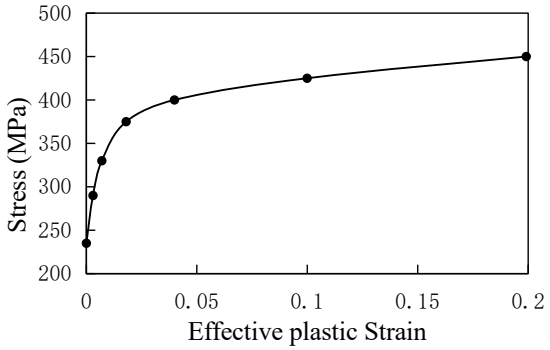

Figure 2: True tress versus effective plastic strain curve.

3.2 Element meshing

The rods are modeled as Beam 161, and each rod is divided into 5 equi-length elements. Joints connecting those rods are modeled as rigid points, while its mass is represented by Mass 166. The impactor is treated as the rigid body and it is simulated with Solid 164.

3.3 Verification of the FE method

A reticulated shell of 0.9m span is taken as an example from Wang's (Wang D. et al, 2011) experimental study. The shell is subjected to an impact of a 6.7kg cylinder free fall from the height of 0.03m at the apex. The FE method used in this paper is applied to the experiment model and the results are compared with that from the original reference, which is listed in Table 2.

Table 2: Result comparison (*Rods around the impact region. See in Wang's (Wang D. et al, 2011) experiment)

Rod number		$M_{1\text{-}2}$*	$M_{1\text{-}4}$*	$M_{1\text{-}6}$*
Maximum axial atress	FE	-52.3	-56.5	-59.2
	Test	-50.9	-55.8	-60.0
Maximum apex displacement	FE	-0.93	-	-
	Test	-0.94	-	-
Minimum apex displacement	FE	0.35	-	-
	Test	0.33	-	-

It can be seen from Table 2 that the FE method used in this paper is quite satisfactory. As a result, it is used to simulated the response of the reticulated shell (scaled-down models as well as the prototype) as follows.

4 NUMERICAL RESULTS

Determining representative strain rates for different parts of the model is essential for MIII. It can be inferred from the continuity of the material that strain rate varies continuously through the rods. For simplicity, each rod is divided into 5 (the same as the element meshing number for rods) equal parts and representative strain rate is acquired from the center of these parts.

Strain rate history in the part adjacent to the apex (point A) of the prototype is depicted in Figure 3 as an example. The maximum strain rate is 1.4820 from the figure, so the representative strain rate is 0.7410. Dividing 0.7410 by γ_l leads to a representative strain rate for the model. If $\gamma_l = 0.1$, then $\dot{\varepsilon}_{\mathrm{m}} = 7.410$. As a result, the scaling factor of density for the part is 1.1645 calculated from the combination of Equation (7) and (9). In a real test, the added mass should be 1.417kg according to Equation (8).

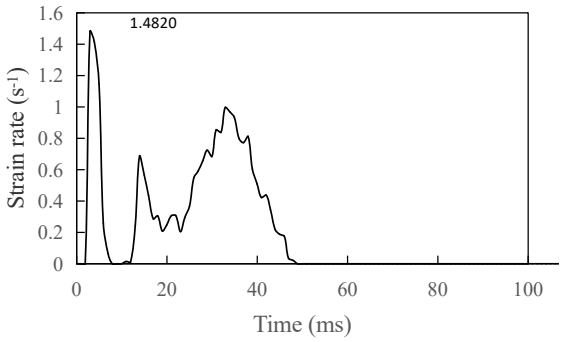

Figure 3: Strain rate history for the part adjacent to the apex.

Representative strain rates in rod 1 through rod 4 of the prototype are reported in Figure 4.

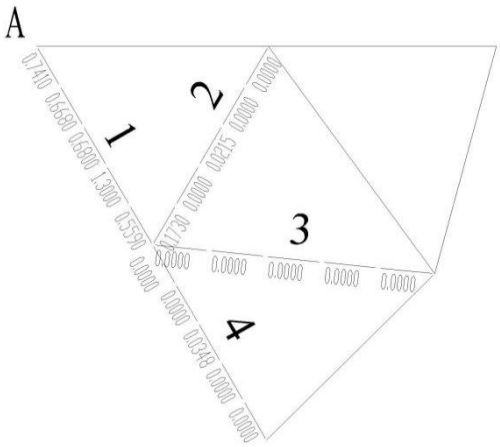

Figure 4: Representative strain rates for the prototype.

Scaled displacements and axial forces are compared between the prototype and the models below:

4.1 Scaling of displacement

Under impact, the dome deforms with a local axisymmetric dimple inside the second ring of latitudinal rods counting from the apex as shown in Figure 5. It is signaled as zone A and can be defined as impact region. The vertical displacements of the outside parts of zone A are less than 14mm for the prototype, thus it can be defined as unimpacted region. The ultimate deformation is best exhibited by depicting the longitudinal rods.

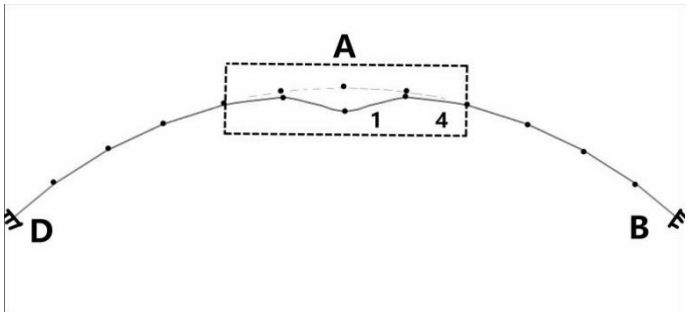

Figure 5: Ultimate deformation of the prototype. (The dashed line denotes the initial state of structure. The solid line denotes the ultimate deformation of the structure.)

Since the deformation of longitudinal rods in plane DAB is axially symmetric and it mainly happens inside the second ring, the displacements of rods 1 and 4 are enough to reflect the structural deformation. It is easy to see that the scaling of displacement equals γ_l. So deformation results for models with MI, MII or MIII scaling should be divided by γ_l to predict deformation in the prototype.

Figure 6 shows the deformation responses of rods 1 and 4. The relative error of the values predicted using MI and MII clearly increases as dimensional scaling factor becomes smaller. The results for MIII are, however, stable and accurate for γ_l=0.1 to 0.01. The predicted deformation profiles for the MIII models almost coincide with those of the prototype. The reduced method (MII) is better than geometrically similar scaling (MI) however. The results using MII are accurate for γ_l=0.1. The relative errors in the apex displacement predicted by MI are beyond 5% for all dimensions, so using it is not suggested.

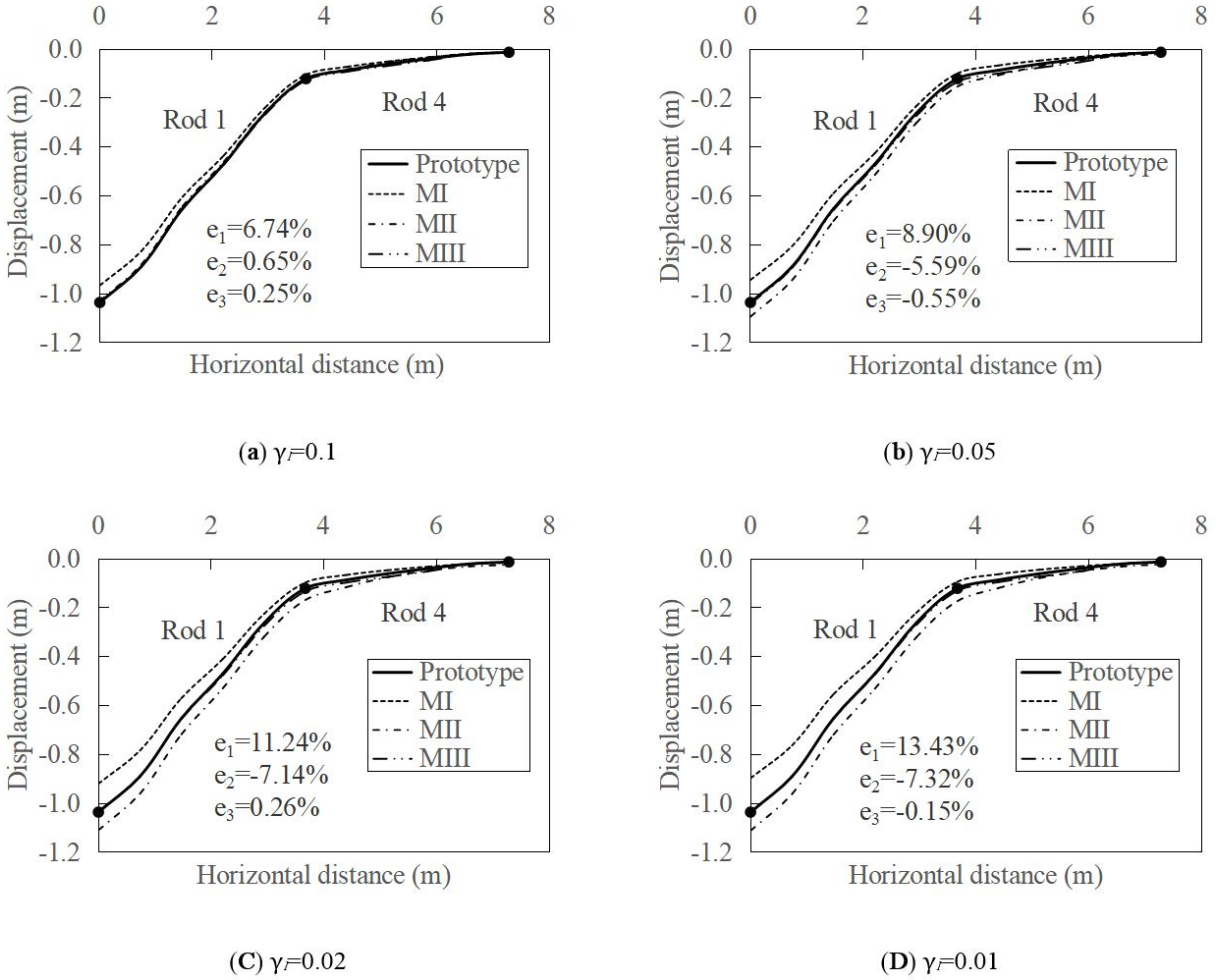

(**a**) γ_l=0.1 (**b**) γ_l=0.05

(**C**) γ_l=0.02 (**D**) γ_l=0.01

Figure 6: Ultimate vertical displacements of rods 1 and 4. e_1, e_2 and e_3 are the relative errors of methods MI, MII and MIII respectively for the apex displacement compared with the prototype.

4.2 Scaling of axial force

An important mechanical behavior for the rods is their axial force history. Rod 1 was taken as an example to evaluate the scaling of axial force history since it is heavily influenced by the impact. Indeed, the maximum axial force appears in rod 1.

Combining Equations (3) and (4) yields

$$\gamma_{\sigma_d} = \gamma_{\sigma_s} g(\dot{\varepsilon}_m) / g(\dot{\varepsilon}_m \gamma_l / \gamma_V) \tag{10}$$

According to dimensional analysis, the scaling factor for axial force can be calculated as

$$\gamma_F = \gamma_l^2 g(\dot{\varepsilon}_m) / g(\dot{\varepsilon}_m \gamma_l / \gamma_V) \tag{11}$$

Since the material is the same for the model and the prototype, $\gamma_{\sigma_s}=1$ and that can be neglected in the equation. The predicted axial force in prototype scale is computed by dividing the model results by γ_F.

Figure 7 depicts axial force histories for rod 1 for the models and the prototype. Positive and negative values refer to pull and push respectively. The response period selected goes from the initial impact time (0s) to 0.2s during which the response is most significant. The maximum axial force appears at the peak of the first wave. For the prototype, the maximum axial force on rod 1 is 424kN. The first wave of the profile predicted by MIII fits well with the prototype for all dimensions, with good agreement for the peak and the trough. The first peak is much larger in the MI model and with MII the first trough is much deeper than in the prototype. Both MI and MII failed to monitor the first and the most important wave. As for the first peak, which is also the maximum during the period, the model by MIII gives an accurate prediction of axial force for all dimensions with relative errors less than 0.20%. Although the relative error of the first peak predicted by MII is no more than 5% for γ_l=0.1, 0.05 and 0.02, the trough value is far lower than in prototype scale, which is unacceptable.

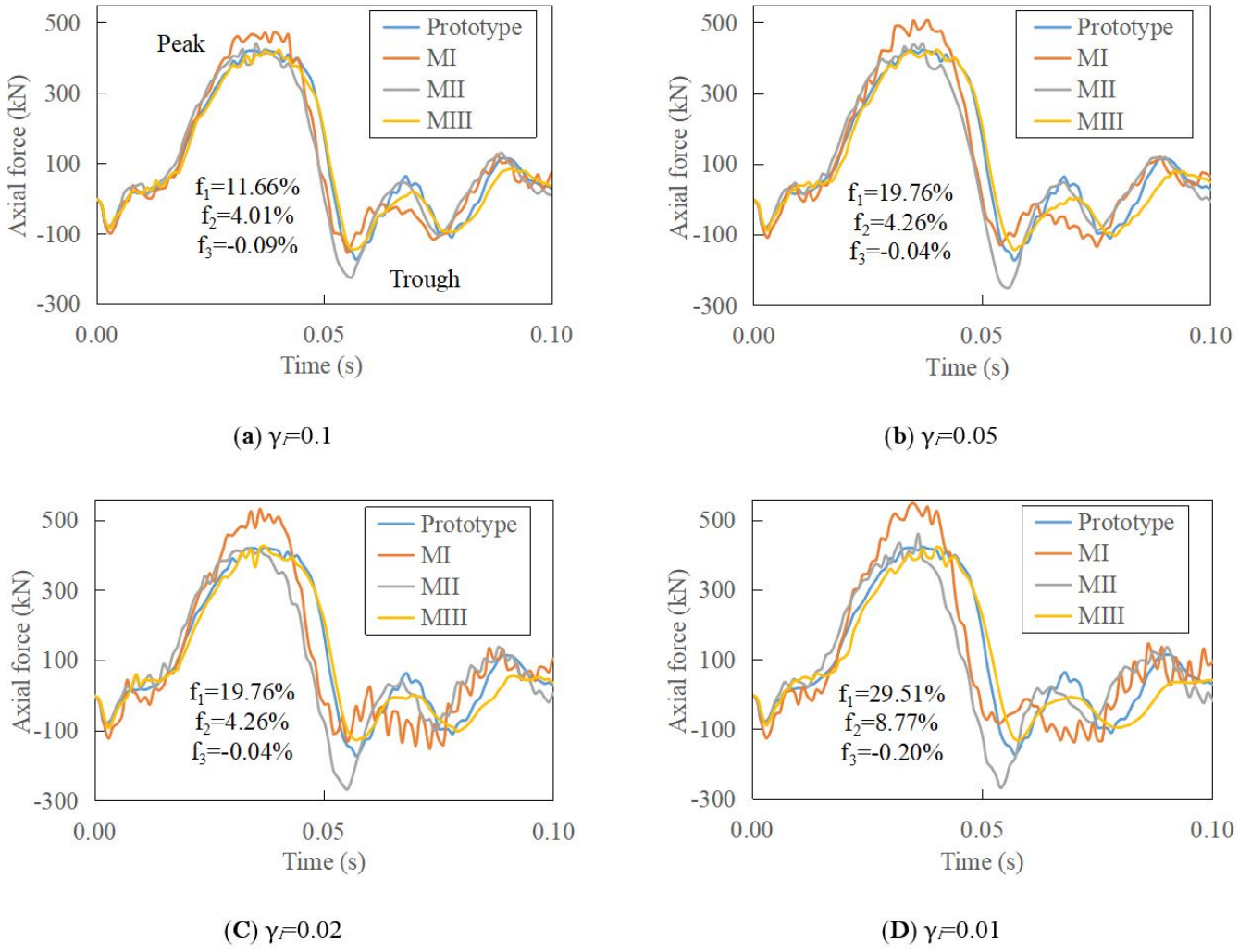

Figure 7: Axial force history for rod 1. f_1, f_2 and f_3 refer to relative errors in the predicted maximum axial force using MI, MII and MIII modelling respectively.

The detailed peak and trough values are listed in Table 3. These extreme values appear in the early stage of the impact history for each rod. Unlike rod 1, however, the trough is absolutely larger than the peak for rods 2, 3 and 4. The results with MIII are generally more stable and accurate than those using the other two methods in terms of both the peak and the trough.

Table 3: Force peaks and troughs (kN).

Scaling Method	γ_l	Rod 1		Rod 2		Rod 3		Rod 4	
		peak	trough	peak	trough	peak	trough	peak	trough
MI	1:10	474	-152	56	-346	36	-113	145	-129
	1:20	509	-133	62	-372	37	-112	159	-141
	1:50	533	-151	67	-370	41	-113	184	-146
	1:100	550	-136	69	-393	52	-120	190	-152
MII	1:10	442	-223	49	-343	36	-117	104	-142
	1:20	443	-248	92	-326	40	-120	107	-153
	1:50	419	-267	77	-322	38	-131	105	-149
	1:100	462	-267	121	-318	41	-117	105	-150
MIII	1:10	424	-143	48	-322	43	-105	112	-122
	1:20	425	-143	50	-320	47	-107	124	-126
	1:50	428	-127	51	-325	51	-109	131	-121
	1:100	424	-130	49	-328	55	-117	133	-113
Prototype		424	-172	45	-317	34	-103	102	-123

5 Discussion

A key principle of dimensional analysis is that variables sharing the same dimension should be scaled equally. However, for the present scaling method (MIII) it is not necessary to alter the elastic modulus E of the material or the static stress σ_s with the dynamic stress σ_d. That is based on the assumption that the structure's deformation is so large that the elastic part can be ignored, so the scaling method can be conceived as partial similitude method.

The tests here were performed using finite element method calculations, but in reality the proposed scaling method should be applied in laboratory tests. The main obstacle is a lack of information about the strain rate in the model. As a result, FEM simulation should be conducted to gather strain rate estimates for each part before a real test. Those strain rate data determine the mass of the impactor and the amount of mass added to each part of the model. For the reticulated dome, since the strain rate effect is important only inside the second ring of latitudinal rods, only the rods inside that range will require additional mass. For simplicity, each rod can be divided into 5 equilong parts and masses added according to the strain rate of that particular part.

Since the strain rate changes with time for each part of the structure, the strain rate used in equations (6)–(8) can be chosen as half of the maximum strain rate. This has been proposed by Perrone and Bhadra (1979, 1984) and it is the only uncertain factor for the MIII scaling procedure. However, we can see through the results that the approximate procedure is good enough with ultimate vertical displacement relative error no more than 0.6% for all scaling cases.

This new scaling method can also be applied by changing the initial impact speed according to Equation (5), as presented in the works of Oshiro & Alves (2009) and Mazzariol & Alves (2014). Several iterations may be need to determine the value of γ_V. Therefore, Equation (8) is rewritten as

$$\Delta m = \rho A_p \left[g(\dot{\varepsilon}_m) / g(\dot{\varepsilon}_m \gamma_l / \gamma_V) - 1 \right] \tag{12}$$

which is the mass that should be added to each component.

Equation (11) relates γ_F with the square of γ_l, indicating a larger error for the force than for the displacement. That explains why the results in Section 4.1 are much better than those in Section 4.2.

6 CONCLUSIONS

A new technique based on partial similitude and dimensional analysis has been proposed. The innovative manipulation is adding mass to components of a structure in model scale to balance varied strain rate effects.

The new technique was tested using the case of an impact on a reticulated dome through using finite element modelling, and the results were compared with those of reduced scaling method (MII) and geometrically similar scaling method (MI). MII only provide an accurate prediction of the rods' displacements for γ_l=0.1 scaling, whereas the new method predicts the rods' displacements well for all of the scale factors tested. MII failed to predict the first wave of axial force for all dimensions, whereas the profile of the new method coincided with that of the prototype.

Geometrically-similar scaling failed to predict either the displacements or the axial force since it doesn't take strain rate effects into consideration. In that point, the new technique significantly broadens the applicability of the scaling method to more complex, strain rate-sensitive impact problems.

References

Alves M., Oshiro R. E. (2006). Scaling the impact of a mass on a structure. International Journal of Impact Engineering 32: 1158-1173.

Booth E., Collier D., Miles J. (1983). Impact scalability of plated steel structures. Structural Crashworthiness 136-174.

Buckingham E. (1914) On physically similar systems: illustrations of the use of dimensional equations [J]. Physical Review 4: 345.

Cowper G. R., Symonds P. S. (1957). Strain-hardening and strain-rate effects in the impact loading of cantilever beams. Small Business Economics 31: 235-263.

Ding B., Lu H., Li X., Liu J., Liu Q. (2015). Experimental study on single-layer cylindrical reticulated shell under impact force. Journal of Vibration Engineering 28: 692-702.

Drazetic P., Ravalard Y., Dacheux F., Marguet B. (1994). Applying non-direct similitude technique to the dynamic bending collapse of rectangular section tubes. International Journal of Impact Engineering 15: 797-814.

Duffey T. A. (1970) Scaling laws for fuel capsules subjected to blast, impact, and thermal loading. Sandia Labs., Albuquerque, N. Mex.

Fan F., Wang D., Zhi X., Shen S. (2010). Failure modes of reticulated domes subjected to impact and the judgment. Thin Walled Structures 48: 143-149.

Jackson K. E. (1994). Workshop on Scaling Effects in Composite Materials and Structures. Scaling Effects in Composite Materials and Structures. Hampton, VA, United States.

Johnson W. (1972). Impact strength of materials. Edward Arnold, London.

Jones N. (1987). Scaling of inelastic structures loaded dynamically, Monash University, Melbourne, Australia.

Jones N. (2011). Structural impact. Cambridge University Press.

Li H., Guo K., Wei J., Qin D. Q. (2006). The dynamic response of a single-layer reticulated shell to drop hammer impact. Explosion and Shock Waves 26:39.

Lin L., Sun Y., Zhi X., Yin H. (2015). Dynamic response of the single-layer kiewitt-8 reticulated dome subjected to the airplane crash. Halong Bay, Vietnam. Proceedings of the 2015 International Conference on Intelligent Transportation, Big Data and Smart City. Institute of Electrical and Electronics Engineers Inc. 339-342.

Mazzariol L. M., Alves M. (2014). Scaling the impact of a mass on a plate using models of different materials. 4th International conference on impact of lightweight structures–ICILLS 2014, Cape Town, South Africa.

Ministry of Construction (2014). Code for design of steel structures. GB 50017-2014.

Nevill G. E., (1963). Similitude studies of re-entry vehicle response to impulsive loading. Southwest Research Institute Report. No. AF SWC-TDR-63-1.

Oshiro R. E., Alves M. (2009). Scaling of structures subject to impact loads when using a power law constitutive equation. International Journal of Solids and Structures 46: 3412-3421.

Perrone N., Bhadra P. (1979). A simplified method to account for plastic rate sensitivity with large deformations [J]. Journal of Applied Mechanics 46: 811-816.

Perrone N., Bhadra P. (1984). Simplified large deflection mode solutions for impulsively loaded, viscoplastic, circular membranes. Journal of Applied Mechanics 51: 505-509.

Shokrieh M. M., Askari A. (2013). Similitude Study of Impacted Composite Laminates under Buckling Loading. Journal of Engineering Mechanics 139: 1334-1340.

Soedel W. (1971). Similitude Approximations for Vibrating Thin Shells. Journal of the Acoustical Society of America 48.

Viot P., Ballère L., Guillaumat L. and Lataillade J. L. (2008). Scale effects on the response of composite structures under impact loading. Engineering Fracture Mechanics 75: 2725-2736.

Wang D., Fan F., Zhi X., Shen S. (2011). Experimental study on single-layer reticulated dome under impact. Journal of Building Structures 32: 34-41.

Wang X., Lei J. (2012). Calculation model on single layer lattice shell static and dynamic impact analysis. Xi'an, China. Advanced Materials Research. Trans Tech Publications 62-65.

Wang X., Ma X., Liang Y., Wu C. (2016). Test research on dynamic behavior of single-layer reticulated dome subjected to inclined impact loads. Journal of Vibration, Measurement and Diagnosis 36: 445-450.

Wei D., Hu C. (2015). Impact response of single-layer lattice shells. Journal of Tianjin University Science and Technology 48: 127-133.

Westine P. S., Dodge F. T., Baker W. E. (1973). Similarity methods in engineering dynamics. Spartan Books. Hayden Book Co..

Wisnom M. R. (1999). Size effects in the testing of fibre-composite materials. Composites Science & Technology, 59: 1937-1957.

Wu C., Wang X. L., Liang Y. X., Yin Z. Z. (2014). Dynamic response of reticulated domes under the impact, Hangzhou, China. Applied Mechanics and Materials. Trans Tech Publications Ltd 58-61.

Xu Z., Yang F., Guan Z. W. (2016). An experimental and numerical study on scaling effects in the low velocity impact response of CFRP laminates. Composite Structures 154: 69-78.

Yang F. J., Hassan M. Z., Cantwell W. J. (2013). Scaling effects in the low velocity impact response of sandwich structures. Composite Structures 99: 97-104.

Zhao Y. (1998). Suggestion of a new dimensionless number for dynamic plastic response of beams and plates [J]. Archive of Applied Mechanics 68: 524-538.

Zheng L. (2012). Finite element analysis of a single-layer reticulated dome and the suspendome under impact loading, Yichang, China. Advanced Materials Research. Trans Tech Publications 844-848.

Zheng L., Chen Z. (2011). Finite element analysis of a single-layer reticulated dome under impact loading. Guangzhou, China. Advanced Materials Research. Trans Tech Publications 327-331.